

See discussions, stats, and author profiles for this publication at: <https://www.researchgate.net/publication/200028945>

# Aqueous Coordination Chemistry of Quinoline-Based Fluorescence Probes for the Biological Chemistry of Zinc

ARTICLE *in* JOURNAL OF THE AMERICAN CHEMICAL SOCIETY · DECEMBER 1999

Impact Factor: 12.11 · DOI: 10.1021/ja992709f

---

CITATIONS

210

---

READS

114

## 2 AUTHORS:



**Christoph J Fahrni**

Georgia Institute of Technology

49 PUBLICATIONS 3,260 CITATIONS

SEE PROFILE



**Thomas Vincent O'Halloran**

Northwestern University

181 PUBLICATIONS 14,101 CITATIONS

SEE PROFILE

# Aqueous Coordination Chemistry of Quinoline-Based Fluorescence Probes for the Biological Chemistry of Zinc

Christoph J. Fahrni<sup>†</sup> and Thomas V. O'Halloran<sup>\*,†,‡</sup>

Contribution from the Department of Chemistry and Department of Biochemistry, Molecular Biology, and Cell Biology, Northwestern University, 2145 Sheridan Road, Evanston, Illinois 60208

Received July 30, 1999

**Abstract:** Metal-specific fluorescence probes are of increasing importance in understanding the neurobiology and general cell biology of zinc. Several quinoline-based compounds such as TSQ and zinquin have been employed to detect zinc in fluorescence microscopy experiments in vivo; however, the aqueous solution chemistry remains equivocal. In some cases, this family of probes is said to reveal labile pools of Zn(II) inside the cell, yet in other cases, these probes are suggested to remove Zn(II) from tightly bound sites in proteins. Since the binding modes, coordination numbers, and thermodynamics of zinc–zinquin interactions in aqueous solution have not been established, these proposals are difficult to distinguish. Here we show that, under physiological conditions, the various forms of zinquin bind Zn(II) with a high degree of cooperativity forming 2:1 complexes. Potentiometric, UV–visible, and fluorescence methods all yield an overall binding constant of  $\log K = 13.5$  under physiological conditions. To put this number in perspective with other Zn chelators and biological ligands, we compare the calculated so-called pM values ( $-\log[\text{Zn(II)}]_{\text{free}}$ ) for a series of compounds with different stoichiometries under a typical condition. The pZn value for zinquin (9.3) is similar to that of EGTA (9.5) but much smaller than the value for carbonic anhydrase (12.4) or EDTA (14.3) and, thus, serves as a useful gauge for comparing zinc affinities. With respect to in vivo applications of zinquin, such as intracellular fluorescence microscopy studies, we find that the typical detection limit for free Zn(II) in aqueous solution is 4 pM, or 0.3 parts per trillion, at pH 7.2. These results have implications for the availability of zinc in various intracellular compartments.

## Introduction

Zinc is an abundant component of most living cells. The total concentration of this element in an undifferentiated mammalian cell is in the millimolar range;<sup>1</sup> however, the details of chemical speciation and compartmentalization are not well established. Members of all five classes of enzymes are known to employ zinc in catalysis or structure stabilization;<sup>2</sup> it is not known how they acquire zinc inside the cell. While metallothionein has been implicated in both Zn homeostasis and metal detoxification,<sup>3–9</sup> its role in activating apoenzymes in vivo remains an open issue. Transport proteins involved in uptake and intracellular trafficking of zinc are just beginning to emerge.<sup>10–12</sup> The importance

of zinc-specific fluorescent probes is particularly apparent in understanding zinc chemistry in the brain,<sup>13</sup> where stimulated release of this metal ion from zincergic neurons in the hippocampus is thought to be important in some aspects of neurotransmission.<sup>14,15</sup> As more roles for nonenzymatic zinc pools become apparent, so has the need for well-characterized cell permeant chemical probes of zinc biology.

Various fluorescence-based zinc probes have recently been developed. Some of these are fluorescent adducts of Zn-chelating peptides<sup>16–18</sup> and proteins<sup>19</sup> while others are dye adducts of Zn-chelating macrocyclic compounds.<sup>20,21</sup> Zinc chelators based on a quinoline core, such as 6-methoxy-(8-*p*-toluenesulfonamido)-quinoline (TSQ), are currently the most widely used zinc-activated fluorophores. Unlike peptide-based probes, the quinoline compounds are generally cell permeant and can readily

\* To whom correspondence should be addressed. Phone: 847-491-5060. Fax: 847-491-7713. E-mail: t-ohalloran@nwu.edu.

<sup>†</sup> Department of Chemistry.

<sup>‡</sup> Department of Biochemistry, Molecular Biology, and Cell Biology.

(1) Suhy, D. A.; O'Halloran, T. V. In *Metal-responsive gene regulation and the zinc metalloregulatory model*; Sigel, A., Sigel, H., Eds.; Marcel Dekker: Basel, Switzerland, 1996; Vol. 32 (Interactions of Metal Ions with Nucleotides, Nucleic Acids, and Their Constituents), p 557.

(2) Vallee, B. L.; Falchuk, K. H. *Physiol. Rev.* **1993**, 73, 79.

(3) Müller, H. P.; Brugnera, E.; Georgiev, O.; Badzong, M.; Müller, K. H.; Schaffner, W. *Somat. Cell Mol. Genet.* **1995**, 21, 289.

(4) Radtke, F.; Heuchel, R.; Georgiev, O.; Hergersberg, M.; Gariglio, M.; Dembic, Z.; Schaffner, W. *EMBO J.* **1993**, 12, 1355.

(5) Zeng, J.; Heuchel, R.; Schaffner, W.; Kägi, J. H. R. *FEBS Lett.* **1991**, 279, 310.

(6) Suhy, D. A.; Simon, K. D.; Linzer, D. I. H.; O'Halloran, T. V. *J. Biol. Chem.* **1999**, 274, 9183.

(7) Maret, W.; Jacob, C.; Vallee, B. L.; Fischer, E. H. *Proc. Natl. Acad. Sci. U.S.A.* **1999**, 96, 1936.

(8) Palmiter, R. D. *Proc. Natl. Acad. Sci. U.S.A.* **1998**, 95, 8428.

(9) Kelly, E. J.; Quaife, C. J.; Froelick, G. J.; Palmiter, R. D. *J. Nutr.* **1996**, 126, 1782.

(10) Eng, B. H.; Gueriot, M. L.; Eide, D.; Saier, M. H. *J. Membr. Biol.* **1998**, 166, 1.

(11) Palmiter, R.; Cole, T.; Findley, S. *EMBO J.* **1996**, 15, 1784.

(12) Cole, T. B.; Wenzel, H. J.; Kafer, K. E.; Schwartzkop, P. A.; Palmiter, R. D. *Proc. Natl. Acad. Sci. U.S.A.* **1999**, 96, 1716.

(13) Budde, T.; Minta, A.; White, J. A.; Kay, A. R. *Neuroscience* **1997**, 79, 347.

(14) Canzoniero, L. M. T.; Sensi, S. L.; Choi, D. W. *Neurobiol. Dis.* **1998**, 4, 454.

(15) Choi, D. W.; Koh, J. Y. *Annu. Rev. Neurosci.* **1998**, 21, 347.

(16) Walkup, G. K.; Imperiali, B. *J. Org. Chem.* **1998**, 63, 6727.

(17) Walkup, G. K.; Imperiali, B. *J. Am. Chem. Soc.* **1997**, 119, 3443.

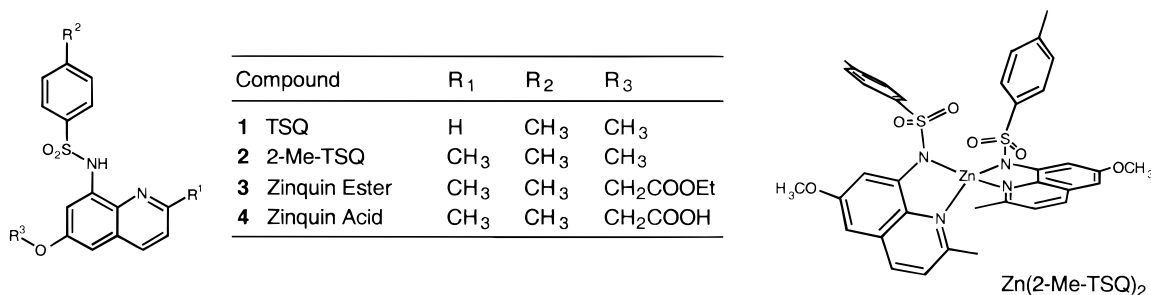
(18) Godwin, H. A.; Berg, J. M. *J. Am. Chem. Soc.* **1996**, 118, 6514.

(19) Thompson, R. B.; Maliwal, B. P.; Fierke, C. A. *Anal. Chem.* **1998**, 70, 1749.

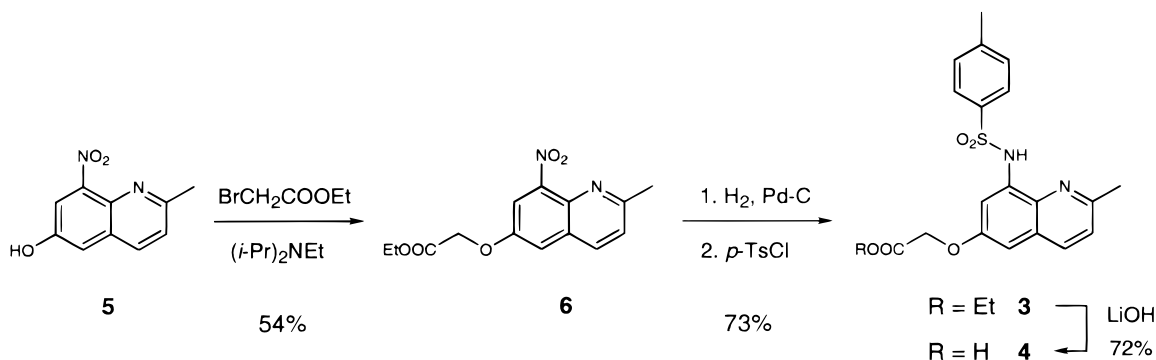
(20) Koike, T.; Watanabe, T.; Aoki, S.; Kimura, E.; Shiro, M. *J. Am. Chem. Soc.* **1996**, 118, 12696.

(21) Fabbrizzi, L.; Licchelli, M.; Pallavicini, P.; Taglietti, A. *Inorg. Chem.* **1996**, 35, 1733.

Chart 1



Scheme 1



be applied to many living systems. For example TSQ was initially employed in physiological staining of the mossy fibers of the hippocampus, a region of the brain that exhibits elevated concentrations of zinc.<sup>22–24</sup> The TSQ derivative zinquin was designed with an extra methyl group and an ester, the latter to purportedly improve the cellular retention.<sup>25</sup> The Zn specificity of zinquin and its comparatively low toxicity make it a powerful qualitative probe for the *in vivo* investigation of the intracellular chemistry of labile zinc ions. It has been used to visualize some intracellular zinc pools in apoptosis,<sup>26,27</sup> in zinc-accumulating pancreatic islet cells,<sup>25</sup> and in growth of undifferentiated eukaryotic cells.<sup>1,11,12</sup>

To develop a more quantitative understanding of changes in intracellular zinc, we have investigated the thermodynamics of zinc binding to several vital quinoline-based chelators under physiological conditions (Chart 1). Little is known about the aqueous solution chemistry of zinquin. Differences in estimates for the zinc affinity of zinquin can be found in the literature.<sup>25,26,28,29</sup> Most of the studies of the Zn-binding equilibria are in mixed organic solvent–water systems and come to the conclusion that zinquin is sensitive to nanomolar Zn(II). To establish the affinities of zinc and copper for this class of bidentate chelators in aqueous solution, we have undertaken a

series of potentiometric, fluorescence, and UV-based approaches to establish the equilibrium constants in aqueous media under physiological buffer conditions. Each of these methods leads to the same conclusion: this probe can readily detect free Zn(II) at a concentration of 4 pM under conditions such as those employed in typical microscopy experiments on living cells. These measurements thus provide a starting point for understanding the changes in zinc concentrations in various cellular compartments and for the further development of the next generation of vital probes for Zn(II).

## Results

**Synthesis.** The synthesis of zinquin ester (**3**) and some derivatives has been recently reported.<sup>29,30</sup> We describe here a modified three-step synthesis starting from 6-hydroxy-8-nitroquinoline **5**, which we also use as a versatile precursor for the synthesis of several other zinquin derivatives (Scheme 1).<sup>30</sup> Nucleophilic substitution with ethyl bromoacetate gave best yields (54%) in acetonitrile and with diisopropylethylamine as base. Subsequent hydrogenation of the nitro group with either Pt or Pd on activated carbon as catalyst gave essentially pure amine **7** in 86% yield. Reaction with *p*-toluenesulfonyl chloride in pyridine at 0 °C gave the zinquin ester (**3**) under mild conditions in 85% yield. The procedure can be readily scaled up and provides an easy access to gram quantities of zinquin ester (**3**). Some potentiometric and spectroscopic studies were carried out using the acid form **4** of zinquin, which was obtained in 72% yield by hydrolysis with lithium hydroxide in a methanol–THF–water solvent mixture.

**Potentiometric Studies.** The accuracy of potentiometry<sup>31</sup> is often superior to other methods such as spectrophotometry, calorimetry, or NMR spectroscopy. In most systems it provides the most reliable stability constants; however, UV–visible

(22) Frederickson, C. J.; Kasarskis, E. J.; Ringo, D.; Frederickson, R. E. *J. Neurosci. Methods* **1987**, *20*, 91.

(23) Frederickson, C. J.; Perez-Clausell, J.; Danscher, G. *J. Histochem. Cytochem.* **1987**, *35*, 579.

(24) Frederickson, C. J. *Int. Rev. Neurobiol.* **1989**, *31*, 145.

(25) Zalewski, P. D.; Millard, S. H.; Forbes, I. J.; Kapaniris, O.; Slavotinek, A.; Betts, W. H.; Ward, A. D.; Lincoln, S. F.; Mahadevan, I. J. *Histochem. Cytochem.* **1994**, *42*, 877.

(26) Zalewski, P. D.; Forbes, I. J.; Seamark, R. F.; Borlinghaus, R.; Betts, W. H.; Lincoln, S. F.; Ward, A. D. *Chem. Biol.* **1994**, *1*, 153.

(27) Zalewski, P. D.; Forbes, I. J.; Betts, W. H. *Biochem. J.* **1993**, *296*, 403.

(28) Hendrickson, K. M.; Rodopoulos, T.; Pittet, P. A.; Mahadevan, I.; Lincoln, S. F.; Ward, A. D.; Kurucsev, T.; Duckworth, P. A.; Forbes, I. J.; Zalewski, P. D.; Betts, W. H. *J. Chem. Soc., Dalton Trans.* **1997**, 3879.

(29) Mahadevan, I. B.; Kimber, M. C.; Lincoln, S. F.; Tiekink, E. R. T.; Ward, A. D.; Betts, W. H.; Forbes, I. J.; Zalewski, P. D. *Aust. J. Chem.* **1996**, *49*, 561.

(30) Nasir, M. S.; Fahrmi, C. J.; Suhy, D. A.; Kolodnick, K. J.; Singer, C. P.; O'Halloran, T. V. *J. Biol. Inorg. Chem.*, in press.

(31) Martell, A. E.; Motekaitis, R. J. *The Determination and Use of Stability Constants*; VCH: New York, 1988.

methods are less cumbersome and can be applied to systems involving low solubility. We performed our initial analysis of the zinquin–Zn(II) equilibrium system using potentiometry and subsequently applied UV–visible and fluorescence methods for studies under physiological conditions.

Potentiometric measurements are usually carried out in aqueous solution using commercially available glass electrodes, with ligand and metal ion concentrations between 2 and 5 mM; lower concentrations can give rise to irreproducible potentials. Due to the somewhat low solubility of zinquin ester (**3**), the potentiometric measurements were performed in a mixture of dimethyl sulfoxide (DMSO) and H<sub>2</sub>O (80:20 w/w), a solvent that has been already widely used in potentiometry.<sup>32–34</sup> The solvent components have a mole fraction of 0.5, and the excellent solubility properties of DMSO are essentially preserved. The dielectric constant ( $\epsilon = 72$ ) is only slightly lower than that of water; thus this mixture readily dissolves ionic solutes and also prevents significant ion-pair formation. Additionally, the large pH range (up to 18.4)<sup>35</sup> and the significantly lower hygroscopic character compared to pure DMSO are also favorable. The potential of a simple commercially available glass electrode with Ag/AgCl reference is highly reproducible and shows Nernstian response over a wide range.<sup>35</sup> Typically, a solution of the ligand (2–3 mM) was titrated with 0.05 M KOH at constant ionic strength (0.1 M KClO<sub>4</sub>) for the determination of the pK values. In a second run, the same titration was performed in the presence of 1 or 2 equiv of zinc(II) triflate (Figure 1). The measured emf data were processed with the program BEST<sup>31</sup> using the equilibrium models discussed in the following paragraph, providing the corresponding protonation and complex formation constants (Table 1).

**(a) Zinquin Ester (3).** The release of the sulfonamide proton of zinquin ester (**3**) (hereafter referred to as simply zinquin) occurs with a pK of  $9.32 \pm 0.02$ . This value is slightly lower than the pK of the corresponding 6-methoxy-substituted derivative<sup>30</sup> ( $9.63 \pm 0.02$ ; see Table 1), reflecting the enhanced electron-withdrawing character of the ethoxycarbonylmethyl substituent. To evaluate the protonation constant of the quinoline nitrogen, titrations were performed in the presence of 1 molar equiv of aqueous HClO<sub>4</sub>. The initially measured pH indicated no significant protonation of the quinoline nitrogen. The first pK is thus below 2, and it was therefore not considered in the equilibrium model for data analysis. While the overall binding constant  $\log \beta_2$  corresponding to the 2:1 complex could be measured with high reliability ( $\log \beta_2 = 17.54 \pm 0.02$ ), the  $\log \beta_1$  value of 7 is not well determined and must be considered an upper limit. A detailed analysis of the experimental data suggested that the occurrence of this species under the given conditions is too low to be reflected in the shape of the titration curve. The overall error ( $\sigma$ ) of the corresponding curve fit is completely independent of  $\log \beta_1$  in the range between 0 and 7; however,  $\sigma$  increases rapidly as trial values of  $\log \beta_1$  exceed 7. Therefore, the stability constant of the 1:1 complex ( $\log \beta_1$ ) must be equal or lower than 7. As a consequence, the difference between  $\log \beta_2$  and  $\log \beta_1$ , which corresponds to the formation constant of the 2:1 complex ( $\log K_2$ ), must be greater than 10. The formation of the 2:1 complex is thus favored by at least 3 orders of magnitude over the formation of a simple 1:1 complex.

(32) Faus, J.; García-España, E.; Marcelino, V.; Bencini, A.; Bianchi, A. *Inorg. Chim. Acta* **1990**, 172, 203.

(33) García-España, E.; Ballester, M.-J.; Lloret, F.; Moratal, J. M.; Faus, J.; Bianchi, A. *J. Chem. Soc., Dalton Trans.* **1988**, 101.

(34) Lloret, F.; Mollar, M.; Faus, J.; Julve, M.; Castro, I.; Diaz, W. *Inorg. Chim. Acta* **1991**, 189, 195.

(35) Georgieva, M.; Velinov, G.; Budevsky, O. *Anal. Chim. Acta* **1977**, 90, 83.

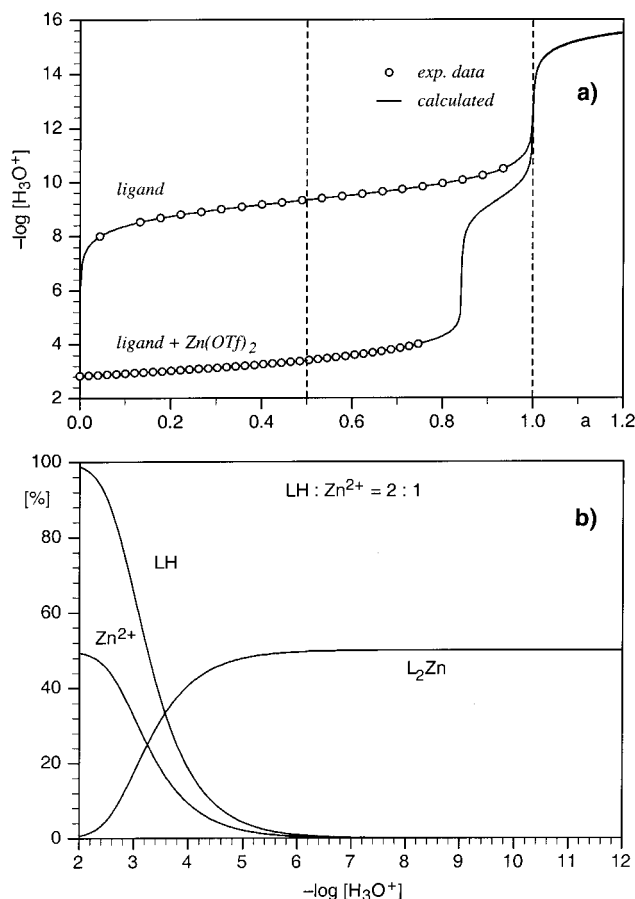


**Figure 1.** (a) Potentiometric equilibrium curves of zinquin ester (**3**) in the absence and presence of 0.5 mol equiv of Zn(II) in DMSO–H<sub>2</sub>O (80:20 w/w,  $\mu = 0.1$  M KClO<sub>4</sub>, 25 °C). a, moles of base added per mole of ligand present; concentration of ligand, 5.3 mM. (b) Species distribution diagram as a function of  $-\log[\text{H}_3\text{O}^+]$  for a system containing 2.5 mM Zn(II) and 5 mM **3**.

**Table 1.** Equilibrium Data for Protonation and Complex Formation of Quinoline Fluorophores with Zn(II) in DMSO–H<sub>2</sub>O (80:20 w/w, 0.1 M KClO<sub>4</sub>, 25 °C)

ligand	reaction	formation constant (log K)
2-Me-TSQ ( <b>2</b> ) <sup>30</sup>	$\text{L}^- + \text{H}^+ = \text{LH}$	$9.63 \pm 0.02$
	$\text{LH} + \text{H}^+ = \text{LH}_2^+$	<2
	$\text{L}^- + \text{Zn}^{2+} = \text{ZnL}^+$	$8.43 \pm 0.38$ (log $\beta_1$ )
	$2\text{L}^- + \text{Zn}^{2+} = \text{ZnL}_2$	$18.24 \pm 0.02$ (log $\beta_2$ )
zinquin ester ( <b>3</b> )	$\text{L}^- + \text{H}^+ = \text{LH}$	$9.32 \pm 0.02$
	$\text{LH} + \text{H}^+ = \text{LH}_2^+$	<2
	$\text{L}^- + \text{Zn}^{2+} = \text{ZnL}^+$	<7 (log $\beta_1$ )
	$2\text{L}^- + \text{Zn}^{2+} = \text{ZnL}_2$	$17.54 \pm 0.02$ (log $\beta_2$ )
zinquin acid ( <b>4</b> )	$\text{L}^{2-} + \text{H}^+ = \text{LH}^-$	$9.91 \pm 0.02$
	$\text{LH}^- + \text{H}^+ = \text{LH}_2$	$5.77 \pm 0.03$
	$\text{LH}_2 + \text{H}^+ = \text{LH}_3^+$	<2
	$\text{L}^{2-} + \text{Zn}^{2+} = \text{ZnL}$	<8 (log $\beta_1$ )
	$2\text{L}^{2-} + \text{Zn}^{2+} = \text{ZnL}_2^{2-}$	$18.43 \pm 0.07$ (log $\beta_2$ )
	$\text{L}^{2-} + \text{Zn}^{2+} + \text{H}^+ = \text{ZnLH}^+$	<14
	$2\text{L}^{2-} + \text{Zn}^{2+} + \text{H}^+ = \text{ZnL}_2\text{H}^-$	$24.67 \pm 0.04$
	$2\text{L}^{2-} + \text{Zn}^{2+} + 2\text{H}^+ = \text{ZnL}_2\text{H}_2$	$30.19 \pm 0.05$

A species distribution diagram based on the described equilibrium model was calculated (Figure 1), which shows that above physiological pH the 2:1 complex ZnL<sub>2</sub> is the only species present. (The occurrence of a metal hydroxo species was also considered. Using such an extended equilibrium model for the curve-fitting procedure did not affect the overall standard deviation, which suggests that the pK of water coordinating to any 1:1 complex is high and can be neglected here.)



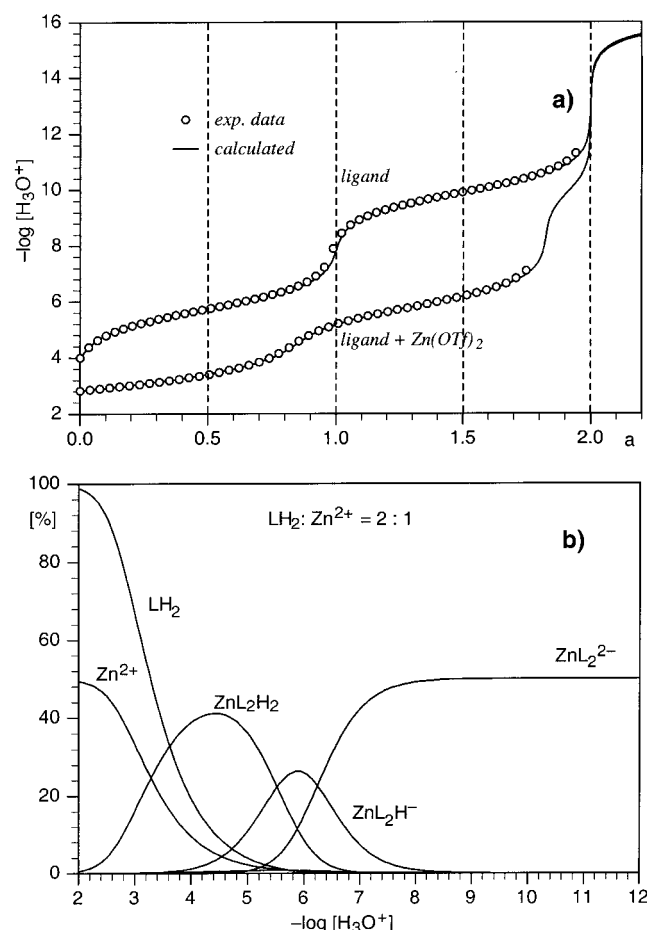


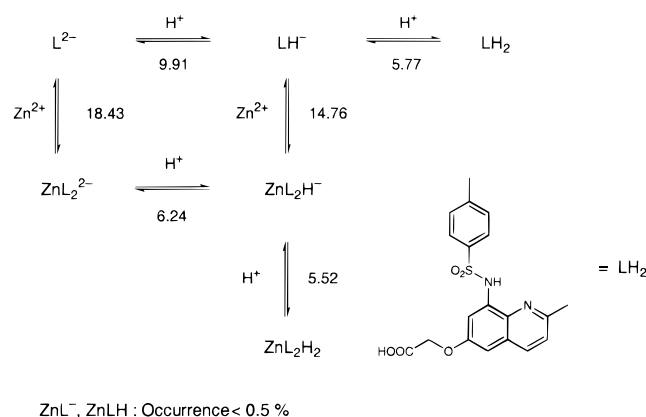
**Figure 2.** (a) Potentiometric equilibrium curves of zinquin acid (**4**) in the absence and presence of 0.5 mol equiv of Zn(II) in DMSO–H<sub>2</sub>O (80:20 w/w,  $\mu = 0.1$  M KClO<sub>4</sub>, 25 °C). *a*, moles of base added per mole of ligand present; concentration of ligand, 5.5 mM. (b) Species distribution diagram as a function of  $-\log[\text{H}_3\text{O}^+]$  for a system containing 2.5 mM Zn(II) and 5 mM **4**.

**(b) Zinquin Acid.** The free acid **4** was also titrated with 0.05 M KOH in DMSO–H<sub>2</sub>O (80:20) and constant ionic strength of 0.1 M KClO<sub>4</sub> (Figure 2). An extra equivalent of perchloric acid was added in order to measure the *pK* of the quinoline nitrogen. As already observed for zinquin ester, the initial pH indicated full dissociation of this proton ( $\text{p}K_1 < 2$ ). Deprotonation of the carboxylic acid proton occurs with a *pK* of  $5.77 \pm 0.03$ , and the loss of the sulfonamide proton corresponds to  $\text{p}K = 9.91 \pm 0.02$ . This protonation constant is greater compared to the ester form of zinquin ( $\text{p}K = 9.32$ ), as expected when a negatively charged carboxylate is present in the molecule.

The simulated curve for the titration of ligand **4** in the presence of 1 equiv of Zn(OTf)<sub>2</sub> (see Figure 2) was obtained using the model depicted in Scheme 2. The overall stability constant for the formation of the double negatively charged 2:1 complex ( $\log \beta_2 = 18.43 \pm 0.07$ ) is slightly greater than the constant for the ester **3** ( $17.54 \pm 0.02$ ). This is also in agreement with the trend in proton affinity of the sulfonamide nitrogen (see Table 1), which is also higher for the acid form **4**.

As with the ester form of zinquin, the formation constant of the 1:1 species with the acid form **4** can only be estimated as an upper limit. Nevertheless, on the basis of the titration data, it was possible to evaluate a maximum  $\log \beta_1$  value of 8, which still tolerates a curve fit with low standard deviation. The occurrence of the 1:1 species is simply too low (<0.5%) to be reflected in the shape of the measured titration curve. We

## Scheme 2



conclude that the formation constants of the 1:1 and 2:1 Zn–zinquin acid complexes differ by at least 2 orders of magnitude (Table 1). The calculated species distribution diagram depicted in Figure 2 reflects this: the two 2:1 complexes  $\text{ZnL}_2\text{H}^-$  and  $\text{ZnL}_2^{2-}$  are the only species with significant concentrations in the physiological pH range.

**(c) Copper Affinity of Zinquin.** Copper is an essential element, and Cu(II) typically binds more tightly to nitrogen-containing ligands than Zn(II). It is important to consider the copper affinity of putative Zn(II) probes. The overall formation constant of the Cu(II)–zinquin complex is  $\log \beta_2 = 18.3 \pm 0.05$  and is thus less than one log unit greater than the corresponding Zn(II) complex. This is interesting because Cu(II) complexes of nitrogen-rich ligands are typically many orders of magnitude more stable than the corresponding Zn(II) complexes. Examination of the structure of the Zn(II) complex with the TSQ derivative **2** provides some insights into the surprising parity of Zn(II) and Cu(II) affinities.<sup>30</sup> As a *d*<sup>9</sup> transition metal, Cu(II) preferably adopts a square planar or tetragonally distorted octahedral coordination geometry. While the TSQ and zinquin bite angle of 83° accommodates formation of a stable square planar or octahedral complex, the presence of a methyl group in the 2-position of zinquin hinders formation of a bis- or tris-chelate complex with either of these two geometries. A tetrahedral geometry, on the other hand, relieves the steric interaction between the 2-methyls of adjacent zinquin ligands. A distorted tetrahedral coordination mode is energetically less favorable for Cu(II). These steric aspects of zinquin force the less favorable distorted geometry on the bound metal ion. We conclude that the lower than expected affinity for Cu(II) is in part due to a steric clash of the methyl group in the 2-position of zinquin. The methyl group may increase selectivity of zinquin for the *d*<sup>10</sup> Zn(II) ion, which can readily accommodate the distorted tetrahedral geometry.

**(d) Mixed Solvent vs Aqueous Equilibria.** The equilibrium constants obtained from the studies in DMSO–water mixture do not necessarily correspond to those that apply in pure aqueous solutions. The solvation properties of DMSO, which is an aprotic solvent, are somewhat different from those of water. DMSO has a lower dielectric constant and is a good coordinating agent for cations, but not for anions.<sup>36</sup> The influence of the solvent system on acidity and stability constants has been widely investigated.<sup>32,37,38</sup> On the basis of those studies, *pK* values are

(36) Martin, D.; Hanthall, H. G. *Dimethyl Sulfoxide*; Van Nostrand Reinhold: New York, 1975.

(37) Edward, J. T.; Farrell, P. G.; Kirchnerova, J. *J. Can. Chem.* **1976**, *54*, 1899.

(38) Fini, A.; De Maria, P.; Guarnieri, A.; Varoli, L. *J. Pharm. Sci.* **1987**, *76*, 48.

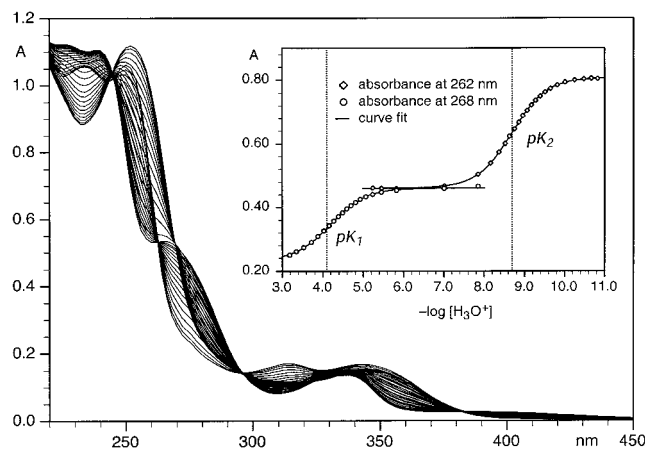


**Figure 3.** UV-visible absorbance of zinquin acid (**4**) as a function of pH (pH range 3–5, 5 mM acetate buffer; pH range 7–10, 5 mM borate buffer,  $\mu = 0.1$  M KCl, 25 °C). Inset: UV-visible absorbance at 262 and 268 nm as a function of pH. Evaluation of the  $pK$  values by nonlinear least-squares fit.

typically 0.2–1 log units higher in DMSO–water (80:20) than in aqueous solution, whereas complexes of Zn(II) have been reported to be 1–4 log units more stable in the mixed solvent. This effect can be attributed to the difference in solvation of the cation in the second coordination sphere. For example, the Zn(II) stability constant of the polyazamacrocyclic [21]aneN7 was determined to be  $\log K = 13.3$  in aqueous solution compared to  $\log K = 17.5$  in DMSO–water (80:20).<sup>32</sup> Accordingly, the higher stability of the 2:1 over the 1:1 complex in DMSO–water is expected to be less pronounced in pure water. The low solubility of zinquin ester (**3**) and acid (**4**) in the pH 1–5 region prevents potentiometric determination of Zn(II) affinity in neat aqueous solution. These equilibria were evaluated by UV spectroscopy and fluorometry. Zinquin acid is readily soluble in aqueous solution at neutral pH. Metal and ligand concentrations for the UV studies were typically in the micromolar range, where ligand and complexes are soluble.

**Determination of the Complex Stability Constant with Zinc under Physiological Conditions.** (a) **Evaluation of  $pK$  Values of Zinquin Acid in Aqueous Solution by UV.** The UV absorption spectra of zinquin acid (**4**) were monitored in solutions in which  $-\log[H_3O^+]$  was varied between 2 and 11 (Figure 3). Two distinct regions were observed, each with a characteristic set of isosbestic points corresponding to the protonation equilibrium of the carboxylic acid and sulfonamide nitrogen, respectively. The two equilibria can be analyzed independently using the corresponding set of absorption traces, which belong to the same set of isosbestic points. Plotting the absorbance against  $-\log[H_3O^+]$  at a constant wavelength allows the evaluation of the  $pK$  value via simple nonlinear curve fitting (Figure 3, inset). The  $pK$  evaluation can principally occur at any wavelength, but since the spectrum set corresponding to the protonation equilibrium of the carboxy moiety shows an isosbestic point at 262 nm, this wavelength allows also the most accurate determination of the molar absorptivity of the single protonated zinquin acid (**4**). The curve fit revealed a  $pK$  value of  $8.68 \pm 0.02$ , which, as expected, is lower than the value measured in the DMSO–water mixture (9.91). Similarly, the set of absorption spectra measured in the pH range between 2.8 and 6.5 gives the  $pK$  value of the carboxylic group (Figure 3, inset). The spectra corresponding to the deprotonation of the sulfonamide nitrogen show an isosbestic point at 268 nm, which was therefore the wavelength of choice for the  $pK$  evaluation of the carboxy group. The corresponding curve fit revealed a

**Table 2.**  $pK$  Values of Zinquin Acid (**4**) in DMSO–H<sub>2</sub>O (80:20 w/w) and Water ( $\mu = 0.1$  M)

solvent	method	
	potentiometry	UV
$pK_1$	DMSO–H <sub>2</sub> O (80:20) $5.77 \pm 0.03$	H <sub>2</sub> O $4.11 \pm 0.03$
$pK_2$	$9.91 \pm 0.02$	$8.68 \pm 0.02$

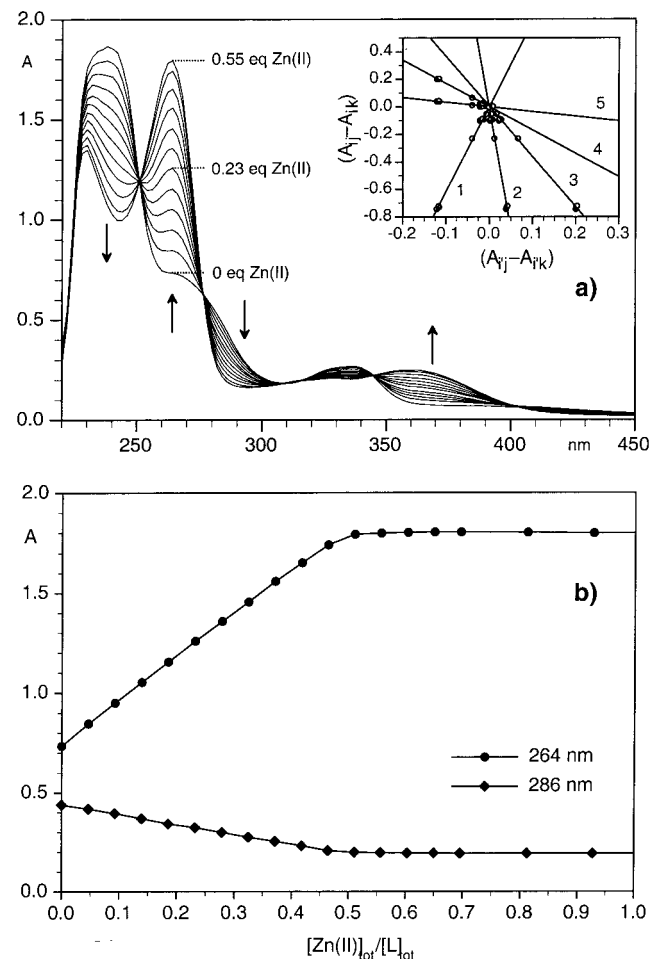


**Figure 4.** (a) UV-visible absorbance of zinquin acid (**4**) as a function of Zn(II) concentration. 40  $\mu$ M of zinquin acid was titrated with 0.05 molar aliquots of zinc(II) triflate (50 mM HEPES buffer, pH 7.20,  $\mu = 0.1$  M KNO<sub>3</sub>, 25 °C). Inset: Two species plot for the UV traces (1:  $i = 260$  nm,  $i' = 370$  nm. 2:  $i = 260$  nm,  $i' = 330$  nm. 3:  $i = 260$  nm,  $i' = 284$  nm. 4:  $i = 284$  nm,  $i' = 370$  nm. 5:  $i = 330$  nm,  $i' = 370$  nm). (b) Absorbance as a function of added Zn(II) monitored at 264 and 286 nm (molar ratio plot).

protonation constant of  $4.11 \pm 0.03$  (a compilation of all measured protonation constants is given in Table 2).

**(b) Stoichiometry of the Metal–Ligand Complex in Aqueous Solution.** The potentiometric studies in DMSO–water solvent mixture are consistent with the 2:1 zinquin–zinc complex as the only species present with significant concentrations at neutral pH. Prior to the UV determination of the zinc binding affinity under physiological conditions, it was important to unambiguously establish the solution composition. Is the 2:1 complex still the only species present or does the 1:1 complex contribute with a substantial amount? A UV titration was carried out by addition of zinc(II) triflate to a HEPES-buffered solution (pH 7.2) of zinquin acid (**4**) in water. The measured absorption spectra (Figure 4a) exhibit a set of well-defined isosbestic points at 250, 276, 310, 316, 344, and 402 nm, which is consistent

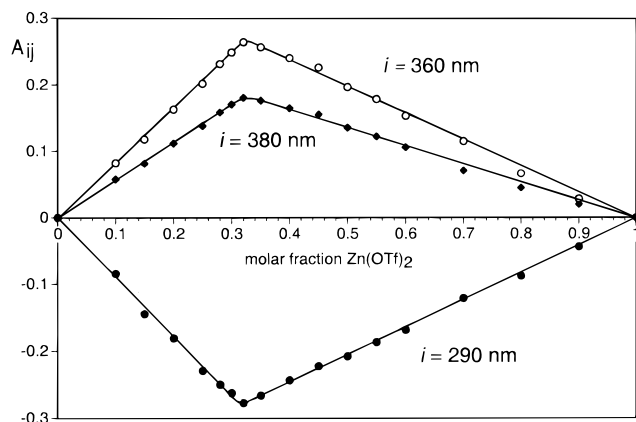


**Figure 5.** Job's plot of zinquin acid (**4**) in 50 mM HEPES buffer (pH 7.20,  $\mu = 0.1$  M  $\text{KNO}_3$ ). The sum of the concentrations of ligand and zinc(II) triflate is 75  $\mu\text{M}$ . The observed absorbance is plotted at three different wavelengths and corrected by the absorbance of total zinquin acid present.

with the presence of only two UV-active species. Since  $\text{Zn}(\text{OTf})_2$  does not absorb in this region, we assume that the two species are free ligand and  $\text{Zn}(\text{II})$ –ligand complex. Furthermore, the number of species present under these conditions can be evaluated using graphical procedures.<sup>39,40</sup> When the equilibrium system has only two states and when the ratio of differences of absorptivities is constant as the medium is changed, plots of  $(A_{ij} - A_{ik})$  versus  $(A_{i'j} - A_{i'k})$  will give straight lines passing through the origin. Here  $A_{ij}$  and  $A_{ik}$  are defined as the absorptivity at wavelength  $i$  and solution compositions  $j$  and  $k$ , respectively, with  $i \neq i'$  and  $j \neq k$ . Such a plot of the absorptivity data from the former titration confirms the occurrence of only two species (Figure 4a, inset). This is also in agreement with the molar ratio graph depicted for wavelengths 264 and 286 nm (Figure 4b). Due to the high binding affinity of zinquin, the absorption at 264 nm increases almost linearly until a ligand-to-metal ratio of 2:1 is reached. Further addition of  $\text{Zn}(\text{II})$  did not affect the absorption spectrum.

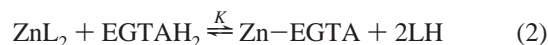
Another approach to unveil the nature of species present is the method of continuous variation (Job's method<sup>41</sup>). A series of solutions are prepared such that the sum of total metal and ligand molar concentrations is constant.

$$[\text{Zn}(\text{II})]_{\text{total}} + [\text{L}]_{\text{total}} = C \quad (1)$$

If the absorbance of a solution at a given wavelength is plotted against mole fractions of metal or ligand, the maximum absorbance yields a value for  $x_{\text{max}}$ , which corresponds to the stoichiometry of the species formed in solution. Thus, an  $x_{\text{max}}$  value of 0.5 would correspond to the formation of a 1:1 complex. The experiment was carried out with zinquin acid (**4**) in HEPES-buffered solution at pH 7.20 (0.1 M  $\text{KNO}_3$ ). The result is shown in Figure 5 and reveals an  $x_{\text{max}}$  of 0.33, which corresponds unambiguously to the formation of a 2:1 complex. Since the  $x_{\text{max}}$  value of 0.33 was obtained at several different wavelengths, the exclusive formation of a 2:1 complex is strongly supported for all of the zinc and ligand concentrations employed in the equilibrium constant determinations. This result is in good agreement with the potentiometric studies in which no 1:1 species was detected and the 2:1 complex is the predominant

species in solution at neutral pH. The data analysis of the following binding studies were therefore restricted to a single complex equilibrium among the 2:1 species, the free metal, and ligand.

**(c) Determination of  $\log \beta_2$  in Aqueous Buffer by Competitive Binding with EGTA.** The UV titration data depicted in Figure 4 show that  $\text{Zn}(\text{II})$  binds very tightly to zinquin acid (**4**) under these conditions. Throughout this titration the added  $\text{Zn}(\text{II})$  is quantitatively bound to the ligand. Thus, the fractional saturation defined by the ratio of formed complex and added zinc is always greater than 99%. As shown by Deranleau<sup>42,43</sup> and Norheim,<sup>44</sup> the relative error in the determination of the binding constant  $K$  is minimized by working in a fractional saturation range between 20 and 80%. Below or above these limits the error will increase exponentially. Since there is essentially no information about  $K_{\text{eq}}$  in data obtained with a fractional saturation close to 0 or 100%, it is not possible to extract a reliable value for the binding constant from the data in Figure 4. The measurement of dissociation constants in the picomolar range or lower can generally be accomplished using a second ligand (e.g. EGTA) with well tuned metal affinity. The equilibrium is then defined by



and with the equilibrium constant

$$K = \frac{[\text{Zn-EGTA}][\text{LH}]^2}{[\text{ZnL}_2][\text{EGTAH}_2]} = \frac{K'_{\text{EGTA}}}{K'_{\text{zinquin}}} \quad (3)$$

$K'$  refers to the apparent binding constant at a given pH and ionic strength and can be calculated from the tabulated absolute binding constants (vide supra).<sup>45</sup> Given  $K$  and the zinc binding constant of the competitor ligand (EGTA), the zinc binding affinity for zinquin can readily be calculated. The binding affinity of the competitor ligand must be carefully chosen, to fulfill the above requirements for the position of the equilibrium. As discussed below, EGTA meets these criteria.

The zinc binding affinity of EGTA is pH dependent and can be calculated for any given pH using published  $\text{pK}$  and  $\log \beta$  values. As Martell and Smith<sup>46</sup> noted, the tabulated figures for protonation constants must be corrected upward by 0.11 when working in 0.1 M ionic strength. This correction is necessary since the tabulated  $\text{pK}$  values are determined using concentrations and not the activity of the hydrogen ion. According to the National Bureau of Standards, pH is defined as  $-\log(a_{\text{H}})$ , where  $a_{\text{H}}$  is 0.78  $c(\text{H}^+)$  at 0.1 M ionic strength. Thus, the tabulated  $\text{pK}$  values for EGTA (9.40, 8.79, 2.66, 2.0) are corrected to 9.51, 8.90, 2.77, and 2.11. The apparent stability constant of  $\text{EGTA-Zn}(\text{II})$  for any given pH can be calculated using Schwarzenbach's  $\alpha$ -coefficient method.<sup>47</sup> In general, the "apparent" or "conditional" stability constant  $K'$  is defined by

$$K' = K_{\text{ML}'} = [\text{ML}]/[\text{M}'][\text{L}'] \quad (4)$$

In this expression,  $[\text{M}']$  refers to the concentration of all the metal ions in solution that have not reacted with the complexing

(42) Deranleau, D. A. *J. Am. Chem. Soc.* **1969**, *91*, 4044.

(43) Deranleau, D. A. *J. Am. Chem. Soc.* **1969**, *91*, 4050.

(44) Norheim, G. *Acta Chem. Scand.* **1969**, *23*, 2808.

(45) Perrin, D. D.; Dempsey, B. *Buffers for pH and Metal Ion Control*; John Wiley & Sons: Chapman and Hall: New York, London, 1974.

(46) Martell, A. E.; Smith, R. M. *NIST Critical Stability Constants of Metal Complexes. NIST Standard Reference Database 46, Version 5.0, 1998.*

(47) Schwarzenbach, G. *Complexometric Titrations*; Interscience Publisher: New York, 1957.

(39) Hartley, F. R.; Burgess, C.; Alock, R. M. *Solution Equilibria*; John Wiley & Sons: New York, 1980.

(40) Connors, K. A. *Binding Constants*; John Wiley & Sons: New York, 1987.

(41) Job, P. *Ann. Chim. (Paris)* **1928**, *9*, 113.



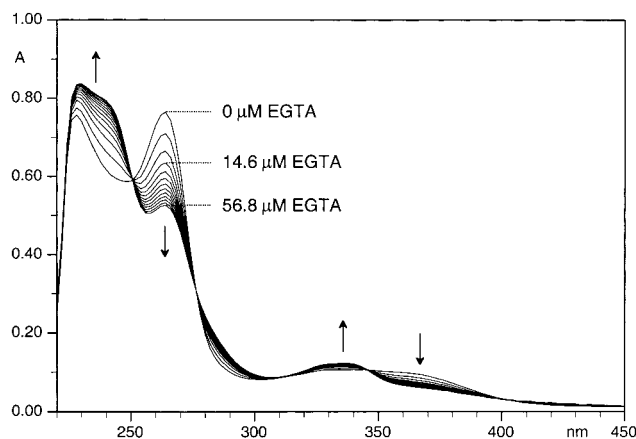


**Figure 6.** UV-visible traces for the titration of 31.5  $\mu\text{M}$  zinquin acid (**4**) and 9.47  $\mu\text{M}$   $\text{Zn}(\text{OTf})_2$  with EGTA (pH 7.20, HEPES; 0.1 M  $\text{KNO}_3$ , 25  $^\circ\text{C}$ ).

agent, thus including metal hydroxo species as well. Analogously,  $[L']$  represents not only the concentration of free ligand but also the concentration of all ligand not bound to the metal. The conditional constant thus gives the relationship between the quantities of interest, namely, the total concentration of uncomplexed metal, the uncomplexed ligand, and the complex formed. Applying Schwarzenbach's  $\alpha$ -coefficients to eq 4 the apparent stability constant  $K'$  can be calculated based on the following equation:

$$K' = K_{\text{ML}}/\alpha_{\text{M}}\alpha_{\text{L}} \quad (5)$$

where

$$\alpha_{\text{M}} = ([\text{M}] + [\text{MOH}] + [\text{M}(\text{OH})_2] + \dots)/[\text{M}]$$

and

$$\alpha_{\text{L}} = ([\text{L}] + [\text{HL}] + [\text{H}_2\text{L}] + \dots)/[\text{L}]$$

Thus, using the tabulated values for the Zn-EGTA system,<sup>46</sup> the apparent binding constant at, for example, pH 7.20 and 0.1 M ionic strength is obtained via the following equation<sup>48</sup> (for details, see also ref 49):

$$\begin{aligned} K'_{\text{ZnEGTA}} &= \frac{K_{\text{ZnEGTA}}(1 + 10^{(\text{p}K_{\text{ZnEGTA}} - \text{pH})})}{(1 + 10^{(\text{pH} - \text{p}K_{\text{Zn}})})(1 + 10^{(\text{p}K_1 - \text{pH})} + 10^{(\text{p}K_1 + \text{p}K_2 - 2\text{pH})})} \\ &= \frac{10^{12.6}(1 + 10^{(-2.13)})}{(1 + 10^{(-1.8)})(1 + 10^{(9.51 - 7.20)} + 10^{(18.41 - 14.40)})} \\ &= 3.78 \times 10^8 \end{aligned} \quad (6)$$

Accordingly, the measured value for  $K'_{\text{zinquin}}$  corresponds to the apparent Zn(II) stability constant under the chosen experimental conditions (pH 7.20 and 0.1 M ionic strength). With the knowledge of the  $\text{p}K$  of zinquin, the absolute stability constant  $K_{\text{zinquin}}$  ( $\beta_2$ ) can then be calculated as described below (eq 7).

**(d) UV Titration of Zinquin Acid-Zn(II) with EGTA.** A HEPES-buffered solution (pH 7.20, 0.1 M  $\text{KNO}_3$ ) of zinc triflate containing 3.3 equiv of zinquin acid (**4**) was titrated with HEPES-buffered EGTA. The UV traces shown in Figure 6 exhibit sharp isosbestic points, suggesting again a single

equilibrium between the free ligand and its 2:1 complex with Zn(II); thus even in the presence of EGTA, only HL and  $\text{ZnL}_2$  species are present at significant levels. The data were analyzed using a nonlinear least-squares fit algorithm (SPECFIT software<sup>50</sup>). Applying the calculated formation constant of  $\log K'_{\text{ZnEGTA}} = 8.58$  to the curve fit, an overall stability constant for the 2:1 zinquin-Zn(II) complex of  $\log \beta_2 = 13.5 \pm 0.1$  was obtained. The indicated uncertainty is based on the published value for the EGTA-Zn(II) complex. With the knowledge of the  $\text{p}K$  values for zinquin in water at 0.1 M ionic strength, the pH-independent (absolute) binding constant is obtained using Schwarzenbach's  $\alpha$ -coefficient method as outlined in eq 7. A compilation of the zinquin acid stability constants is given in Table 3:

$$\log K = \log[K'\alpha_{\text{Zn}}\alpha_{\text{zinquin}}^2] = 16.7 \quad (7)$$

where

$$\alpha_{\text{Zn}} = 1 + 10^{(\text{pH} - \text{p}K_{\text{Zn}})} = 1.016$$

and

$$\alpha_{\text{zinquin}} = 1 + 10^{(\text{p}K - \text{pH})} = 39.9$$

**(e) Fluorescence Titration of EGTA-Zn(II) with Zinquin Acid.** The 2:1 complex of zinquin with zinc exhibits a more than 100-fold greater fluorescence intensity compared to the unbound ligand. On the basis of the Job method analysis above, the presence of a 1:1 complex can be neglected at the concentrations employed here. Thus, the overall fluorescence intensity  $F$  is defined by

$$F = k [\text{ZnL}_2] \quad (8)$$

where  $k$  represents the proportionality constant relating the intensities and concentrations of the species. With the knowledge of the background fluorescence  $F_0$  and the maximum possible fluorescence intensity  $F_\infty$ , the fractional saturation  $f$  can be calculated directly from the measured fluorescence intensity  $F$ :

$$f = (F - F_0)/(F_\infty - F_0) \quad (9)$$

The fluorescence titration experiments were performed by adding aliquots of a zinquin acid (**4**) stock solution to zinc(II) triflate in the presence of various amounts of EGTA (Figure 7). The limiting values for  $F_0$  and  $F_\infty$  were obtained with separate titrations by adding excess ligand to a solution containing no zinc (control) and an identical amount of zinc(II) triflate, respectively. With known total concentrations of Zn(II), EGTA, and zinquin acid (**4**), the equilibrium constant for eq 3 can be directly calculated from the fractional saturation data for each titration point. The average value for the equilibrium constant  $K$  for eq 3 was determined to be  $\log K = 5.11 \pm 0.05$ . Consequently, the log of the apparent stability constant  $K'$  of the  $\text{ZnL}_2$  complex at pH 7.20 and  $\mu = 0.1$  M was calculated to be  $13.7 \pm 0.1$  ( $L$  = zinquin acid **4**). Using the same method described in the preceding paragraph, the pH-independent (absolute) binding constant was calculated to be  $\log \beta_2 = 16.9 \pm 0.1$ , in good agreement with the UV data.

(48) Tsien, R. Y.; Rink, T. J. *Biochim. Biophys. Acta* **1980**, 599, 623.

(49) Tsien, R.; Pozzan, T. *Method. Enzymol.* **1989**, 172, 230.

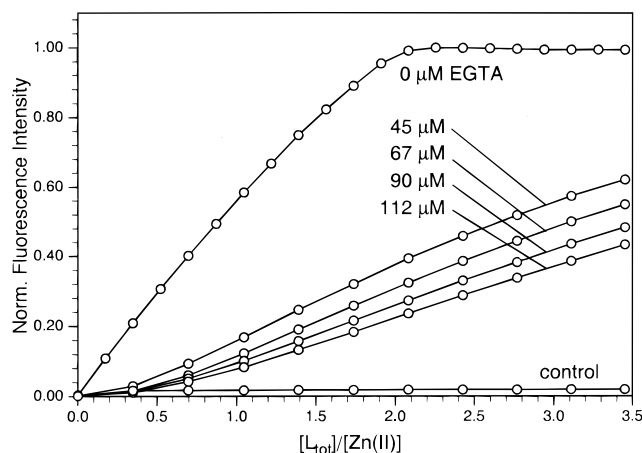
(50) Binstead, R. A.; Zuberbühler, A. D. *SPECFIT Global Analysis System*; 2.10 (rev. X); Spectrum Software Associates: Chapel Hill, NC 27515, 1998.



**Table 3.** Apparent Stability Constant ( $\log K'$ ) and Formation Constant ( $\log \beta_2$ ) of the 2:1 Zinquin Acid–Zn(II) Complex in DMSO–H<sub>2</sub>O (80:20 w/w) and Water ( $\mu = 0.1$  M)

	method			
	potentiometry	competitive binding with EGTA		fluorescence Zn(II)-buffered soln
		UV–visible	fluorescence	
solvent	DMSO–H <sub>2</sub> O (80:20)	H <sub>2</sub> O (pH 7.20)	H <sub>2</sub> O (pH 7.20)	H <sub>2</sub> O (pH 7.20)
$\log K'$ (pH 7.20)		$13.5 \pm 0.1^a$	$13.7 \pm 0.1$	$13.51 \pm 0.03$
$\log \beta_2$	$18.43 \pm 0.07$	$16.7 \pm 0.1^b$	$16.9 \pm 0.1$	

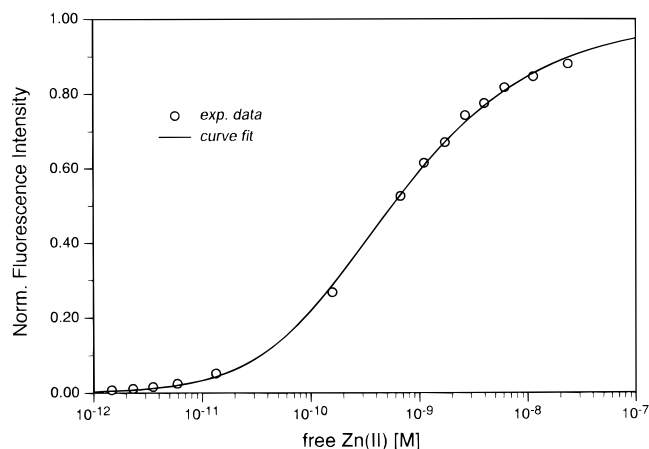
<sup>a</sup> Standard deviation based on uncertainty for  $\log K$  (Zn–EGTA). <sup>b</sup> Calculated on the basis of  $pK$  and  $\log K'$  using Schwarzenbach's  $\alpha$ -coefficient method.<sup>47</sup>

**Figure 7.** Fluorometric titration of zinc(II) triflate (5  $\mu$ M) with zinquin acid (**4**) in the presence of various amounts of EGTA (pH 7.20, HEPES; 0.1 M KNO<sub>3</sub>, 25 °C).

**(f) Determination of the Stability Constant by the Metal-Buffered Solution Method.** To directly determine the sensitivity of zinquin acid (**4**) toward Zn(II) in aqueous solution, a series of metal- and pH-buffered solutions (HEPES, pH 7.2) were prepared. On the basis of the published data for the protonation and complex formation constant of EGTA and HEDTA, the corresponding free Zn(II) concentrations were calculated using an iterative method (program SPE<sup>31</sup>). The measured fluorescence intensities of solutions with identical zinquin acid (**4**) but different free Zn(II) concentrations resulted in a sigmoidal curve from which a zinc binding affinity of  $\log K' = 13.5$  was extracted via nonlinear curve fitting. As before, the presence of a 1:1 complex was not required in the model applied in the curve fit. The fluorescence response of zinquin acid (**4**) as displayed in Figure 8 gives a direct measure for the sensitivity of this probe for Zn(II). Thus, according to Figure 8, the lower detection limit of zinquin acid lies around 4 pM and the fluorescence intensity reaches saturation above 100 nM free Zn(II). Zinquin is therefore optimal for probing free Zn(II) concentrations in the picomolar to nanomolar range. In these experiments, zinquin is 50  $\mu$ M; however, similar results are expected when zinquin is applied to cells at a concentration of 10  $\mu$ M.

## Discussion

The present investigation of the ester and acid forms of zinquin reveals the dye to be sensitive to picomolar concentrations of free Zn(II) and provides insights into the zinquin–Zn(II) equilibrium system under physiological conditions (pH 7.2, 0.1 M ionic strength). A compilation of the measured stability constants determined by UV–visible spectroscopy, potentiometry, and fluorometry for the zinquin acid–Zn(II) complex is given in Table 3. The formation constants determined indepen-

**Figure 8.** Normalized fluorescence intensity of zinquin acid (50  $\mu$ M) as a function of the concentration of free Zn(II) in HEPES buffer (pH 7.20, 0.1 M KNO<sub>3</sub>, 25 °C; 10 mM EGTA or HEDTA, 1–9 mM zinc(II) triflate). Free [Zn(II)] was calculated on the basis of published  $pK$  values and Zn(II) binding constants of EGTA and HEDTA. The fit of the data to eq 10 is shown as a solid line.

dently by these methods in aqueous solution at pH 7.20 are within the experimental error identical.

Potentiometric evaluation of equilibrium constants generally represents the most reliable data. The estimated errors are typically in the range between 5 and 10% (Table 1); however, the low solubility of zinquin in aqueous solution required that the titration be carried out in the mixed DMSO–water solvent system. Extrapolation of the data with respect to a pure aqueous system is only possible to a limited degree (vide supra). This method avoids the need of a competitor ligand, since protonation of the coordinating ligand atoms generally competes with complexation to the metal. This in turn allows the direct analysis of an equilibrium system without additional and potentially interfering ligand. As shown below, the complex stability of the competitor ligand introduces additional uncertainty, whereas the potentiometric determination of equilibrium constants ( $\log \beta$  and  $pK$  values) can readily be accomplished with high accuracy.

The determination of the binding constant in aqueous solution was also accomplished using UV–visible spectroscopy. In general this method is restricted by the sensitivity of the spectrometer, and therefore the dynamic range for the concentration measurement of a chromophore is substantially smaller as compared to potentiometric methods. Additionally, titrations such as these that are carried out at constant pH provide only limited information about the solution chemistry. Given the strong binding affinity of zinquin acid (**4**) toward Zn(II), the stability constant could only be determined in the presence of a competitor ligand. The estimated error of about 25% is thus based on the error of the published binding constant for the competitor ligand (EGTA) and Zn(II).

Among UV–visible spectroscopy, potentiometry, and fluorometry, the latter is the least accurate method for the evaluation of binding constants. Whereas the fluorescence response can be detected at a much lower analyte concentration as compared to UV–visible spectroscopy, the intensity measurements are susceptible to errors arising from photobleaching and intensity fluctuations of the light source.

Since zinquin is a fluorescence probe, the evaluation of the detection limit for Zn(II) by fluorometry was of particular interest. In the case of the UV–visible titration, a preformed Zn(II)–zinquin acid complex was titrated by addition of EGTA, whereas the fluorescence titration was carried out by adding zinquin acid (**4**) to a solution of Zn(II) containing various amounts of EGTA. The substantially different approaches yielded comparable values, underscoring the reliability of the measured stability constants. The stability constant extracted from a series of EGTA- or HEDTA-buffered solutions representing various amounts of free Zn(II) resulted in a value close to the former two methods (Table 3).

The potentiometric results in a DMSO–water solvent mixture as well as the UV spectroscopic investigations in pure water suggest that the 2:1 zinquin–Zn(II) complex is the only species present at significant concentrations at physiological pH in these experiments. This was directly established using two independent methods. First, graphical rank matrix analysis of the titration of zinquin acid with Zn(II) was consistent with a single equilibrium system involving only two UV-active species, unbound and Zn-bound ligand. Second, the Job's plot suggested the formation of a single complex with a 2:1 stoichiometry. The relative abundance of a ZnL complex could become significant at very extreme concentrations of zinc and L (vide infra).

A direct comparison of the aqueous binding affinities measured at pH 7.2 with the critical stability constants ( $\log \beta_2$ ) determined in DMSO–water is not meaningful since the aqueous stability constants are "apparent" and therefore pH dependent. Nevertheless, with the knowledge of the aqueous protonation constants of zinquin acid, the corresponding  $\log \beta_2$  value can be estimated using Schwarzenbach's method<sup>47</sup> (eq 7). Based on the  $\log K'$  value measured via the UV–visible titration, a  $\log \beta_2$  (H<sub>2</sub>O) of  $16.7 \pm 0.1$  was calculated; the fluorescence titration data set yielded a  $\log \beta_2$  (H<sub>2</sub>O) of  $16.9 \pm 0.1$  (see Table 3). The value in DMSO–water is greater by ca. 1.6 log units and is within the expected range. In 50% aqueous ethanol, Hendrickson et al. measured a  $\log \beta_2$  value of  $19.11 \pm 0.06$ ,<sup>28</sup> which is comparable to the binding constant in the DMSO–water solvent mixture ( $\log \beta_2$  (DMSO) =  $18.43 \pm 0.07$ ). In contrast to our studies, Hendrickson et al. reported the presence of a 1:1 complex in EtOH with significant stability ( $\log \beta_1 = 9.65$ ). The data supporting that assignment are not well described, but the discrepancy may arise from the difference in the solvent.

The measured binding constants in DMSO–water together with the equilibrium studies in aqueous solution suggest a highly cooperative behavior of the Zn(II)–zinquin system. This situation is generally observed if the equilibrium constant for coordination of a second ligand is substantially greater than for the 1:1 complex. In this case, the cooperativity may arise as the result of favorable hydrophobic interactions of methyl substituents in the 2-position for a distorted tetrahedral complex (vide infra).<sup>30</sup> As described above, the 1:1 complex is not present at significant levels in any of the performed experiments.

This study delineates the zinquin–Zn(II) equilibrium system under physiological conditions and defines the binding mode and net charge in various states. These conclusions provide a starting point for understanding the chemical species involved in intracellular fluorescence that can ultimately be related to

the cell biology of zinc. The data in Table 3 indicate that the ZnL<sub>2</sub> complex will be the dominant species in solution except under extreme conditions of high Zn(II) and low zinquin (i.e., when [zinquin]  $\sim$  nM and [Zn]<sub>free</sub> > 0.1 mM). These conditions are unlikely when this cell permeant probe is used at 10  $\mu$ M, a concentration typically employed in microscopy experiments. We thus suggest that the majority of the intracellular fluorescence in cells treated with **3** arises from the 2:1 zinquin–Zn(II) complex.

The membrane permeant, unhydrolyzed ester (**3**), apparently passes through both the plasma membrane and the intracellular membranes and binds free Zn(II) wherever it is available in the cell. The punctate nature of this pattern is consistent with the existence of vesicles that have elevated concentrations of free Zn(II) relative to the rest of the cell. We suggest that the bis(zinquin)–Zn(II) complex in either the acid or ester form is not membrane permeant. Thus, once the complex is formed within a cellular compartment, it is trapped until zinquin dissociates from Zn(II). This scenario accounts for the fact that 6-methoxy-substituted 2-methyl-TSQ (**2**), lacking a hydrolyzable ester group, gave rise to a similar staining pattern.<sup>30</sup> It is likely that the ZnL<sub>2</sub> complex of zinquin ester is the chemical species responsible for the observed staining of distinct intracellular zinc-enriched compartments in published studies.<sup>1,11,25</sup>

**Zinc Specificity.** As expected from the Irving–Williams series, Cu(II) complexes with nitrogen donor ligands are typically found to be more stable than Zn(II) complexes by several orders of magnitude. The difference in binding affinity of zinquin toward Zn(II) and Cu(II) is less than 1 log unit and therefore surprisingly low. A recent structural study of the ZnL<sub>2</sub> complex (L = 2-Me-TSQ, **2**) reveals that this is most likely due to two types of geometric restrictions imposed by the ligand: a comparatively small bite angle and the methyl group in the 2-position of the quinoline ring.<sup>30</sup> In contrast, macrocyclic ligands provide a conformationally less flexible ligand framework. Macrocycles are ideal for the selective coordination of alkali or alkali earth metals, which can be discriminated from each other solely on the basis of their ionic radii and charge, but may be less useful for discrimination between the almost identical ionic radii of Cu(II) and Zn(II). This is reflected in the relative binding affinity of a macrocyclic Zn(II) ligand for Cu(II), where the latter is favored by 15 orders of magnitudes.<sup>51</sup> In that case, the interference with Cu(II) ions in the fluorescence response must be masked with a copper binding protein (bovine serum albumin). Hence, a ligand framework, which is more flexible than a macrocycle but which imposes significant steric restrictions upon metal coordination geometry, appears to be the most promising approach for the design of Zn(II)-selective fluorescence probes.

**Comparison of the Zn(II) Affinity with Various Ligands.** The overall stability constant of the zinquin acid–Zn(II) complex (Table 3) suggests strong binding, but how does this compare to the affinity of other biological ligands, including Zn–protein complexes? The direct comparison of the binding constant, for example, with EDTA ( $\log K = 14.5$ , pH 7.2, 0.1 M ionic strength) can be misleading. EDTA binds Zn(II) with a 1:1 stoichiometry, whereas zinquin forms a 2:1 complex, and therefore the units of the corresponding binding constants are different. For a given complex equilibrium system, the concentration of unbound metal cation represents a direct gauge of the ligand–metal affinity with consideration of all involved equilibria. Thus, comparison of the free metal concentration, typically referred to as  $pM = -\log[M]$ ,<sup>45</sup> allows a direct comparison of various ligands regardless of their binding stoichiometry. Since the  $pM$  depends on total ligand and metal concentration, pH, temperature, and ionic strength of the

(51) Kimura, E.; Koike, T. *Chem. Soc. Rev.* **1998**, 27, 179.

**Table 4.** Calculated pZn Values ( $-\log[\text{Zn}]_{\text{free}}$ ) for a Solution Containing 10  $\mu\text{M}$  the Indicated Ligand, 1  $\mu\text{M}$  Zn(II) at pH 7.0, 0.1 M Ionic Strength, and 25  $^{\circ}\text{C}$ 

ligand	pZn	ligand	pZn
NTA	9.0	TPEN	16.0
EGTA	9.5	zincuin acid	9.3
EDTA	14.3	carbonic anhydrase	12.4 <sup>a</sup>

<sup>a</sup> Calculation based on  $\log K = 11.4$  (see ref 52).

solution, a comparison is only meaningful for a predefined set of these parameters. The pZn data compiled in Table 4 were calculated for an equilibrium system containing 10  $\mu\text{M}$  total ligand (a concentration typically used in vivo assays), 1  $\mu\text{M}$  Zn(II) at pH 7.2, 25  $^{\circ}\text{C}$ , and 0.1 M ionic strength. Under these conditions, the Zn(II) affinity of zinquin acid with a pZn of 9.3 is comparable to the affinity of NTA or EGTA with pZn of 9.0 and 9.5, respectively. Thus, EDTA and zinc enzymes such as carbonic anhydrase<sup>52</sup> bind Zn(II) with substantially higher affinity corresponding to a pZn of 14.3 and 12.4, respectively. Since the defined pM conditions are very similar to those defined by fluorescence microscopy experiments in vivo, we conclude that these quinoline-based probes do not mobilize Zn(II) from enzymes such as carbonic anhydrase.

As a simple measure for the intrinsic brightness of a fluorophore, the product of its extinction coefficient and quantum efficiency is commonly reported. A value of  $1.6 \times 10^3 \text{ M}^{-1} \text{ cm}^{-1}$  was estimated for zinquin under Zn(II)-saturated conditions (370 nm) and is thus comparable to the commercially available Ca(II)-specific probe fura-2 with a quantum efficiency extinction coefficient product between  $5 \times 10^3$  and  $1.6 \times 10^4 \text{ M}^{-1} \text{ cm}^{-1}$  (340 nm).<sup>53</sup> However, unlike fura-2, zinquin is not a ratiometric probe, and in the absence of Zn(II), zinquin is essentially nonfluorescent. Nevertheless, using a variety of methods, the solution chemistry data establish a lower detection limit of zinquin acid for free Zn(II) around 4 pM, at which concentration the fluorescence intensity increases by about 5 times over the background fluorescence. Above 100 nM free Zn(II) the fluorescence intensity reaches saturation. Assuming an optimal dynamic range of 20–80% fractional saturation, zinquin is an ideal fluorophore for probing free Zn(II) concentrations between 100 pM and 10 nM. Furthermore, on the basis of the experimentally determined dynamic range of zinquin, we conclude that the concentration of labile or free Zn(II) in the observed intracellular vesicles<sup>30</sup> must be greater than 100 pM.

## Experimental Section

**Synthesis. Material and reagents:** 4-amino-3-nitrophenol (Aldrich, 98%), crotonaldehyde (Aldrich, 99%, predominantly trans), ethyl bromoacetate (Aldrich, 98%), Pd on activated carbon (Aldrich, 5 wt %), *p*-toluenesulfonyl chloride (Aldrich, 99%). NMR:  $\delta$  in ppm vs SiMe<sub>4</sub> (0 ppm, <sup>1</sup>H, 300 MHz), CDCl<sub>3</sub> (77.0 ppm, <sup>13</sup>C, 75 MHz). MS: selected peaks; *m/z*. IR: (CHCl<sub>3</sub> or KBr): selected bands in  $\text{cm}^{-1}$ , br = broad. Flash column chromatography (FC): Merck silica gel (70–230 mesh). TLC: 0.25 mm, Merck silica gel 60 F254, visualizing at 254 nm or with 2% KMnO<sub>4</sub> solution.

**(a) 2-Methyl-6-hydroxy-8-nitroquinoline (5).** A suspension of 10 g (65 mmol) of 4-amino-3-nitrophenol in 75 mL of hydrochloric acid (37%) and 30 g of concentrated phosphoric acid (85%) was heated to 80  $^{\circ}\text{C}$ , and 4.68 g (66.7 mmol) of crotonaldehyde was gradually added within 1 h. The reaction mixture was subsequently stirred at 95  $^{\circ}\text{C}$  for a further 3 h and then cooled to room temperature. The solution was poured on 200 mL of ice–water, 20 mL of concentrated NH<sub>4</sub>OH was added, and the mixture was filtered through a pad of Celite. The filtrate was neutralized with concentrated NH<sub>4</sub>OH solution until the product started to precipitate. The red solid was filtered off, washed with water,

and dried in vacuo affording 6.82 g of a dark red solid (33 mmol, 52%): mp >185  $^{\circ}\text{C}$  (dec); *R*<sub>f</sub> 0.62 (1:1 hexane–EtOAc); <sup>1</sup>H NMR (DMSO-*d*<sub>6</sub>, 300 MHz)  $\delta$  2.62 (s, 3H), 7.44–7.47 (m, 2H), 7.77 (d, *J* = 2.3 Hz, 1H), 8.23 (d, *J* = 8.5 Hz, 1H), 10.74 (s, br, 1H); <sup>13</sup>C NMR (DMSO-*d*<sub>6</sub>, 75 MHz)  $\delta$  24.8, 112.2, 115.4, 123.8, 128.3, 132.4, 134.6, 148.1, 155.4, 157.1; IR (KBr) 3602, 3085, 1627, 1606, 1529, 1361, 1251, 1138, 872, 782  $\text{cm}^{-1}$ ; MS (70 eV) 205 (19), 204 (M<sup>+</sup>, 100), 174 (17), 158 (20), 146 (45), 131 (12), 130 (17), 103 (21), 102 (10), 77 (18), 51 (9); FAB HRMS *m/e* calcd for C<sub>10</sub>H<sub>8</sub>N<sub>2</sub>O<sub>3</sub> 204.0535, found 204.0533.

**(b) Ethyl [(2-Methyl-8-nitroquinolin-6-yloxy)acetate] (6).** A solution of hydroxyquinoline 5 (4.0 g, 19.6 mmol), ethyl bromoacetate (4.3 mL), and diisopropylethylamine (6.8 mL) in 100 mL of anhydrous ethanol was refluxed for 24 h. After cooling to room temperature the mixture was concentrated in vacuo, and the residue dissolved in 300 mL of CH<sub>2</sub>Cl<sub>2</sub> and extracted first with 1 M HCl and then with 5% NaOH. The organic phase was dried (MgSO<sub>4</sub>) and concentrated in vacuo and the residue crystallized from CH<sub>2</sub>Cl<sub>2</sub>–hexane, affording 3.06 g (10.5 mmol, 54%) of ester 6 as colorless needles: mp 139–140  $^{\circ}\text{C}$ ; *R*<sub>f</sub> 0.35 (2:1 hexane–EtOAc); <sup>1</sup>H NMR (CDCl<sub>3</sub>, 300 MHz)  $\delta$  1.31 (t, *J* = 7.2 Hz, 3H), 2.69 (s, 3H), 4.30 (q, *J* = 7.2 Hz, 2H), 4.76 (s, 2H), 7.19 (d, *J* = 2.7 Hz, 1H), 7.34 (d, *J* = 8.6 Hz, 1H), 7.67 (d, *J* = 2.7 Hz, 1H), 7.96 (d, *J* = 8.6 Hz, 1H); <sup>13</sup>C NMR (CDCl<sub>3</sub>, 75 MHz)  $\delta$  14.1, 25.4, 61.7, 65.8, 110.7, 115.6, 124.1, 127.8, 134.8, 135.1, 148.4, 153.4, 159.7, 167.8; IR (KBr) 2988 br, 1744, 1632, 1605, 1536, 1376, 1247, 1205, 1163, 1138, 1077, 860, 780  $\text{cm}^{-1}$ ; MS (70 eV) 292 (3), 291 (20), 290 (M<sup>+</sup>, 100), 232 (10), 217 (24); FAB HRMS *m/e* calcd for C<sub>14</sub>H<sub>14</sub>N<sub>2</sub>O<sub>5</sub> 290.0902, found 290.092.

**(c) Ethyl [(2-Methyl-8-aminoquinolin-6-yloxy)acetate] (7).** A suspension of nitroquinoline 6 (3.0 g, 10.3 mmol) and 300 mg of Pd catalyst (5 wt % on carbon) in 150 mL of EtOH was hydrogenated at ambient temperature for 24 h. The catalyst was filtered off (Celite), washed with EtOH and the filtrate concentrated in vacuo. The residue was filtered through a short silica gel column (4 × 5 cm, 500 mL EtOAc–hexane 1:1), the filtrate concentrated, and the residue crystallized from MeCl<sub>2</sub>–hexane, providing 2.31 g (8.88 mmol, 86%) of pure amine 7 as pale yellow needles: mp 114–115  $^{\circ}\text{C}$ ; *R*<sub>f</sub> 0.44 (2:1 hexane–EtOAc); <sup>1</sup>H NMR (CDCl<sub>3</sub>, 300 MHz)  $\delta$  1.30 (t, *J* = 7.0 Hz, 3H), 2.30 (s, 3H), 2.64 (s, 3H), 4.28 (q, *J* = 7.0, 2H), 4.66 (s, 2H), 6.61 (d, *J* = 2.5 Hz, 1H), 7.18–7.23 (m, 3H), 7.50 (d, *J* = 2.5 Hz, 1H), 7.79–7.84 (m, 3H), 9.3 (s, br, 1H); <sup>13</sup>C NMR (CDCl<sub>3</sub>, 75 MHz)  $\delta$  14.1, 21.4, 24.7, 61.5, 65.5, 101.0, 106.7, 123.3, 126.7, 127.1, 129.5, 134.3, 134.4, 135.2, 136.3, 143.7, 155.4, 155.5, 168.5; IR (KBr) 3252, 2984, 1767, 1607, 1505, 1374, 1341, 1204, 1175, 1160, 1092, 840, 665, 544  $\text{cm}^{-1}$ ; MS (70 eV) 417 (2), 416 (12), 415 (30), 414 (M<sup>+</sup>, 100), 350 (18), 259 (35), 231 (20), 173 (5), 172 (15), 157 (12), 155 (8), 91 (12); FAB HRMS *m/e* calcd for C<sub>21</sub>H<sub>22</sub>N<sub>2</sub>O<sub>5</sub> 414.1249, found 414.1248.

**(d) Ethyl [(2-Methyl-8-*p*-toluenesulfonylaminoquinolin-6-yloxy)-acetate] (3) (zinquin).** A solution of amine 7 (500 mg, 1.92 mmol) in 8 mL of anhydrous pyridine was cooled to 0  $^{\circ}\text{C}$ , and *p*-toluenesulfonyl chloride (549 mg, 2.88 mmol) was added. The mixture was stirred at 0  $^{\circ}\text{C}$  for 2 h and then overnight at room temperature. The reaction mixture was subsequently poured on ice–water (100 mL) and the precipitated product filtered off. Recrystallization of the crude product from EtOH afforded 677 mg (1.63 mmol, 85%) of zinquin (3) as colorless needles. Analytical data were identical with published data.<sup>29</sup>

**(e) Zinquin Acid (4).** To a solution of LiOH·H<sub>2</sub>O (350 mg) in a mixture of H<sub>2</sub>O (4 mL), THF (8 mL), and MeOH (4 mL) was added zinquin ester (3) (200 mg, 0.482 mmol). The reaction mixture was refluxed for 4 h, cooled to room temperature, and diluted with H<sub>2</sub>O (20 mL). Aqueous HCl (1 M) was added until the product started to precipitate. The product was filtered off, washed with a little H<sub>2</sub>O, and dried in vacuo affording 135 mg (0.35 mmol, 72%) of zinquin acid (4) as a colorless solid. Analytical data were identical with published data.<sup>29</sup>

**Potentiometry.** The potentiometric titrations were carried out as described by Lloret et al.<sup>34,54</sup> All potential measurements were performed with an Orion 720A pH meter using an Accu-pHast combination glass microelectrode with Ag/AgCl reference and double junction. Potential readings were reproducible within the instrument's accuracy ( $\pm 0.1$  mV), and the response of the electrode was instantaneous. Measurements were carried out under a N<sub>2</sub> atmosphere (solvent vapor-saturated gas) and at 25  $\pm 0.1$   $^{\circ}\text{C}$  by circulating constant-temperature water through

(52) Kiefer, L. L.; Krebs, J. F.; Paterno, S. A.; Fierke, C. A. *Biochemistry* **1993**, 32, 9896.

(53) Minta, A.; Kao, J. P. Y.; Tsien, R. Y. *J. Biol. Chem.* **1989**, 264, 8171.

(54) Lloret, F.; Moratal, J.; Faus, J. J. *Chem. Soc., Dalton Trans.* **1983**, 1743.



the water-jacketed titration cell. The electrode was dipped into DMSO–water (80:20) for 3 h before use. DMSO was purified by distillation over CaH<sub>2</sub> under reduced pressure and stored under nitrogen in the dark. An accurate concentration of the basic titrant (0.05 M KOH in DMSO–water, 80:20 w/w) was determined by Gran's method<sup>55</sup> with a standardized HCl solution (Aldrich). The electrode potential  $E^\circ$  was determined by titrating HClO<sub>4</sub> solutions of accurately known concentration with KOH. The data were analyzed by Gran's method using the program MAGEC.<sup>56</sup> From a large number of titrations the autoprotolysis constant of water ( $pK_w$ ) was determined to be  $18.46 \pm 0.02$  (25 °C, 0.1 M KClO<sub>4</sub>) and is in good agreement with the published value of  $18.40 \pm 0.02$ .<sup>35</sup> All  $pK_a$  values and stability constants were measured with constant ionic strength (0.1 M KClO<sub>4</sub>). The FORTRAN program BEST<sup>31</sup> was used to process the potentiometric data and calculate both protonation and stability constants.

**Electrode Calibration in Aqueous Solution.** Measurements were performed with a Mettler combination glass electrode (No. 414023002). For the determination of  $pK$  values in aqueous solution, the electrode was calibrated for  $-\log[H_3O^+]$  by titration of a standardized HCl solution (Aldrich, 0.1 N volumetric standard) with KOH (Aldrich, 0.1 N volumetric standard) at 25 °C and 0.1 M constant ionic strength (KCl). The end point,  $E^\circ$ , and slope were determined by Gran's method.<sup>55</sup> For the determination of the stability constants, the electrode was calibrated for pH using commercial pH reference solutions.

**UV–Visible Spectroscopy.** Absorption spectra were recorded at 25 °C using a Hewlett-Packard HP 8452 spectrometer with constant-temperature accessory. Throughout the titrations the sample solution was stirred with a magnetic stirring device. Path length was 1 cm, with a cell volume of 1.0 or 3.0 mL.

**(a) Determination of  $pK$  Values.** The UV absorption spectra of zinquin acid were monitored for a series of solutions, in which the pH was varied between 2 and 11. For  $-\log[H_3O^+]$  concentrations between 3 and 5, an acetate buffer (5 mM sodium acetate–aqueous HCl, 0.1 M KCl) was applied, whereas a borate buffer (5 mM boric acid–NaOH, 0.1 M KCl) was used to prepare solutions for  $-\log[H_3O^+]$  between 7 and 11. The emf of each solution was directly measured in the UV cell with a combination glass electrode, converted to  $-\log[H_3O^+]$  (based on  $E^\circ$  and slope from the calibration), and plotted against the absorbance at 262 (basic region) and 268 nm (acidic region). A nonlinear curve fit with the following formula was applied to compute the corresponding  $pK$  values:

$$A_{\text{obs}} = (A_{\text{max}}(10^{(\text{pH}-\text{pK})}) + A_{\text{min}})/(1 + 10^{(\text{pH}-\text{pK})})$$

**(b) Titration of Zinquin Acid (4) with Zn(OTf)<sub>2</sub>.** To a 60  $\mu\text{M}$  solution of zinquin acid in HEPES buffer (50 mM, pH 7.20, 0.1M KNO<sub>3</sub>) were added 3  $\mu\text{L}$  aliquots of a 4.23 mM aqueous Zn(OTf)<sub>2</sub> stock solution at 25 °C. Upon each addition, the solution was stirred for 30 min to reach equilibrium and the UV–visible spectrum was subsequently monitored. The recorded UV–visible traces were analyzed by a graphical method for determining the number of species in solution.<sup>57</sup> A “two species” test was performed by plotting  $a_{ij} - a_{ij'}$  vs  $a_{rj} - a_{rj'}$ , a family of straight lines passing through the origin (with  $a_{ij}$  referring to the absorbance at wavelength  $i$  with solution composition  $j$ ).

**(c) Job's Plot.**<sup>41</sup> A series of HEPES-buffered solutions (50 mM, pH 7.20, 0.1 M KNO<sub>3</sub>) of zinquin acid and Zn(OTf)<sub>2</sub> were prepared such that the sum of total metal and total ligand molar concentration was constant (75  $\mu\text{M}$ ). The mole fraction of ligand was varied between 0.1 and 1.0. The absorbance of the solutions at 290, 360, and 390 nm were corrected by subtraction of the calculated absorbance of total ligand present and plotted against the molar fraction of the sample.

**(d) Binding Constant Determination by Competitive Binding of Zn(OTf)<sub>2</sub> with Zinquin Acid and EGTA.** A HEPES-buffered solution (50 mM, pH 7.20, 0.1 M KNO<sub>3</sub>) containing zinquin acid (32  $\mu\text{M}$ ) and Zn(OTf)<sub>2</sub> (9.5  $\mu\text{M}$ ) was titrated with 5  $\mu\text{L}$  aliquots of a 2.9 mM solution of EGTA (in HEPES buffer, pH 7.20). Upon each addition of EGTA, the sample solution was stirred for 30 min to reach equilibrium and the UV–visible spectrum was subsequently recorded. The UV–visible

data were analyzed according to the equilibrium model outlined in eq 3 by a nonlinear least-squares fit algorithm using the program SPECFIT.<sup>50</sup>

**Fluorescence Spectroscopy.** Fluorescence spectra and titrations were recorded on a PTI fluorometer (Photon Technology International). To reduce fluctuations of the excitation intensity during the titration, the arc lamp was turned on for at least 60 min prior the experiment. Emission intensities were recorded at 490 nm with an excitation wavelength of 365 nm.

**Binding Constant Determination by Competitive Binding of Zn(OTf)<sub>2</sub> with Zinquin Acid and EGTA.** A HEPES-buffered solution (50 mM, pH 7.20, 0.1 M KNO<sub>3</sub>) containing Zn(OTf)<sub>2</sub> (9.75  $\mu\text{M}$ ) and various amounts of EGTA (0, 45, 67, 90, and 112  $\mu\text{M}$ ) was titrated with 4  $\mu\text{L}$  aliquots of a zinquin acid stock solution (2.55 mM in HEPES, pH 7.20). Upon each addition, the solution was stirred for 30–50 min to reach equilibrium and the fluorescence intensity was subsequently recorded. To avoid photobleaching of the sample, intensity measurements were each performed over a short time period (typically 10 s). The first titration of Zn(OTf)<sub>2</sub> was carried out in absence of EGTA. Under these conditions, zinquin acid forms with Zn(II) quantitatively a 2:1 complex, which therefore allowed calibration of the fluorescence intensity using eq 8. Subsequent titrations were carried out in the presence of various amounts of EGTA. The concentration of formed ZnL<sub>2</sub> complex was then directly calculated from the measured fluorescence intensity according to eq 8. With the knowledge of the total concentration of EGTA, ligand, and Zn(OTf)<sub>2</sub>, the equilibrium constant  $K$  in eq 3 can be calculated for each titration point.

**Detection Limit and Binding Constant Determination of Zinquin Acid for Zn(II) with Metal-Buffered Solutions.** A series of HEPES-buffered solutions (50 mM, pH 7.20, 0.1 M KNO<sub>3</sub>) were prepared containing various amounts of Zn(OTf)<sub>2</sub> (ranging between 1 and 9 mM) and 10 mM of EGTA or HEDTA. The concentration of free Zn(II) was calculated using the program SPE<sup>31</sup> based on the following published  $pK$  and  $\log K$  values for EGTA and HEDTA:<sup>46</sup> (a) EGTA  $pK_1 = 9.40$ ,  $pK_2 = 8.79$ ,  $pK_3 = 2.70$ ,  $\log K (\text{ZnL}) = 12.6$  (25 °C,  $\mu = 0.1$ ); (b) HEDTA  $pK_1 = 9.87$ ,  $pK_2 = 5.38$ ,  $pK_3 = 2.62$ ,  $\log K (\text{ZnL}) = 14.6$  (25 °C,  $\mu = 0.1$ ). All protonation constants were corrected upward by 0.11 to account for 0.1 M ionic strength.<sup>46</sup> Zinquin acid was dissolved in each of these buffer solutions to a final concentration of 50  $\mu\text{M}$ , and after equilibration for 3 h, the fluorescence intensity was monitored. A plot of the measured fluorescence intensity as a function of free Zn(II) concentration allows the calculation of the binding constant ( $\log K = \log \beta_2$ ) via a nonlinear least-squares fit according to the following method. The mass action equation for a 2:1 complex equilibrium is defined by  $[\text{Zn(II)}][\text{L}]^2K = [\text{ZnL}_2]$ . Substitution with the equation for the total ligand concentration  $[\text{L}]_{\text{tot}} = 2[\text{ZnL}_2] + [\text{L}]$  and eq 8 yields an expression for the overall binding constant  $K$ , which is now expressed as a function of free  $[\text{Zn(II)}]$ ,  $[\text{L}]_{\text{tot}}$ , the measured fluorescence intensity  $F$ , and the proportionality constant  $k$ :

$$K = Fk/[\text{Zn(II)}]( [\text{L}]_{\text{tot}}k - 2F )^2 \quad (10)$$

Equation 10 was solved for  $F$  and subsequently applied as a fitting function in the nonlinear least-squares analysis as shown in Figure 8. The quantum efficiency of zinquin ester (3) was measured using 9,10-diphenylanthracene (DPA) as reference compound: The UV absorbance (OD) of an ethanolic DPA solution was adjusted to the absorbance of a solution of the Zn(II)–zinquin 2:1 complex (27  $\mu\text{M}$ ,  $\epsilon = 3850 \text{ M}^{-1} \text{ cm}^{-1}$ ) in EtOH. The fluorescence intensity of each solution was measured with excitation at 370 nm and integrated over the range between 380 and 700 nm. Finally, the product of the integral ratio and the quantum efficiency of DPA ( $\Phi_f = 0.88$ , EtOH)<sup>58</sup> resulted in a quantum efficiency of  $\Phi_f = 0.43$  for the Zn(II)–zinquin 2:1 complex.

**Acknowledgment.** Financial support from NIH (Grants GM38784 and DK52627), the Boughton Trust, and The John S. Guggenheim Foundation, and a postdoctoral fellowship to C.J.F. from the Swiss National Science Foundation is gratefully acknowledged. We thank D. Hung for the mass spectra data, Y. Hitomi and M. Papadopoulou for comments on the manuscript, and D. Suhay for valuable discussions.

JA992709F

(58) Mardelli, O. I. *J. Photochem.* **1977**, 7, 277.

(55) Gran, G. *Analyst (London)* **1951**, 77, 661.

(56) Leggett, D. J. *Computational Methods for the Determination of Formation Constants*; Plenum Press: New York, London, 1985.

(57) Coleman, J. S.; Varga, L. P.; Mastin, S. H. *Inorg. Chem.* **1970**, 9, 1015.